



# **iJRASET**

International Journal For Research in  
Applied Science and Engineering Technology



---

# **INTERNATIONAL JOURNAL FOR RESEARCH**

IN APPLIED SCIENCE & ENGINEERING TECHNOLOGY

---

**Volume: 6      Issue: IV      Month of publication: April 2018**

**DOI: <http://doi.org/10.22214/ijraset.2018.4725>**

**[www.ijraset.com](http://www.ijraset.com)**

**Call: ☎ 08813907089**

**E-mail ID: [ijraset@gmail.com](mailto:ijraset@gmail.com)**

# Optimization and Statistical Analysis of Binary Composite $Y_2O_3/SiO_2$ Prepared by Wet Chemical Route

Navneet Kumari<sup>1</sup>, Dr. Sunil Rohilla<sup>2</sup>

<sup>1</sup>Department of Physics, Mewar University Gangrar, Chittorgarh- 312901 (Rajasthan), India

<sup>2</sup>Materials Science Lab, Department of Applied Physics, TIT&S Engg. College, Birla Colony Bhiwani-127021, India

**Abstract:** Nanopowder binary oxides consisting of Yttrium oxide ( $Y_2O_3$ ) and silicon dioxide ( $SiO_2$ ) was prepared by the chemical co precipitation method. The effect of process variables lattice strain of  $Y_2O_3:SiO_2$  was studied using Central Composite design. The results revealed that the significant factors affecting lattice strain were concentrations and the rate/speed of addition/mixing of precursors, value and duration of annealing temperature. The optimal calculated parameters were found to be annealing temperature  $-300^\circ C$ , drop rate $-20d/min$ , concentration of precursors1 $-1$  (w/v), concentration of precursors2 $-40$  mmol/l, lattice strain  $\approx 0.00121$ . The formation of  $Y_2O_3:SiO_2$  was confirmed by Fourier transform infrared (FTIR) spectroscopy and X-ray diffraction (XRD) studies. The strain values are calculated from W-H plot for annealed samples.

**Keywords:** Nanocomposites, Binary oxides, nanocrystallites, Central composite, nanocrystalline

## I. INTRODUCTION

Nanocomposites containing nanocrystalline rare-earth oxides ( $R_2O_3$ ) and silica have been investigated widely due to their use in many fields. Among various rare-earth oxides,  $Y_2O_3$  (yttria) has recently attracted much attention due to some interesting properties of high thermal stability, conductivity and refractive index [1]. In addition, yttria has been used as one of the potential candidate materials for some functional applications like cathode radiation tubes, anti reflection coating, protection against chemical corrosion, laser amplifier and optical communication [2,3].  $Y_2O_3$  powder had a body-centered cubic structure with an average size of 35 nm, while the  $SiO_2$  powder was amorphous, with narrow size distribution.  $Y_2O_3$  is an excellent luminescent matrix[4]. Exact composition of the intergranular glassy phase is difficult to determine[5]. Due to aggregation of free standing  $Y_2O_3$  nanocrystallites limits its suitability for technological applications. In order to overcome limitations of pure nanocrystalline  $Y_2O_3$ , it has been dispersed in an optically inert and transparent host. From technological point of view, silica matrix is one of the most suitable host matrices for nanocrystallites because of its chemical inertness, ease in getting spherical particles, optically transparency, higher softening temperature and higher thermal shock resistance as well as it supports in growing nanocrystallites of embedded materials [6,7]. The development of new rare-earth oxides and silica binary systems and their characterization are important not only for technological reasons but also for obtaining a better understanding. Literature survey [8-10] reveals that formation of rare-earth oxides/silicates inside or at the surface of amorphous  $SiO_2$  matrix depends on the synthesis method, rare-earth oxide and silica molar ratio and thermal/pressure treatment. "In the present study we report synthesis of  $Y_2O_3-SiO_2$  nano binary oxides.  $Y_2O_3-SiO_2$  composite find uses in a wide variety of applications, such as X-ray imaging, display monitors, laser and amplifiers for fiber-optic communication [11]. The present study, investigates the influence of variables on the nanoparticle properties. the widely useful statistical design for the development and optimization of the relationship between measured variables and a number of independent variables in the form of polynomial equations[12]. Response surface methodology (RSM, combination of mathematical and statistical techniques) has been widely used to acquire the optimal operation conditions for both laboratory and industrial processes [13]. Response surface methodology, one of the most prominent statistical modeling technique. This methodology includes various types of experimental designs such as central composite, 3 level factorial, Box Behnken, D-optimal design, user defined, one factor, miscellaneous and historical data etc., The selection of experimental design is depending on the objectives of the experiment and the number of factors to be investigated. Central Composite design is one of the most popular Response surface designs and advantage of such methodology is to provide less experimental runs and time, thus provides more efficient optimization (Chaudhary et al., 2013; Peng et al., 2013 al., 2014). it is reported by the Montgomery that, The essence of good planning is to design an experiment able

to provide exactly the type of information important for the improvement of the process for obtaining the desired material[14]. In the present study we report synthesis of  $Y_2O_3$ - $SiO_2$  nano binary oxides.  $Y_2O_3$ - $SiO_2$  composite find uses in a wide variety of applications, such as X-ray imaging, display monitors, laser and amplifiers for fiber-optic communication[15].

## II. EXPERIMENTAL DESIGN

For the synthesis of  $Y_2O_3$  via co-precipitation method, oxides of ytterium ( $51 \times 10^{-2}$  mmol) were converted to their chloride salt by adding stoichiometric amount of hot diluted hydrochloric acid after which transparent solution was formed. The ammonxpeia was used as precipitation agent. Then the solution of chloride salt was added to the ammonia solution at a certain rate by means of continuous stirring. The final solution was stirred for 30 minute. The mixture was centrifuged under 2000 rpm for 8 minute. The obtained precipitate was washed with distilled water three times and dried at 80 OC for 24 hours in an electronic oven. The final powder was heated at 800 OC for 30 minutes to complete the phase transformation to  $Y_2O_3$ .

### A. Characterization of sample

Complementary methods were used to characterize annealed samples. In order to determine the crystallite size and lattice constant, XRD patterns of samples were recorded by using a Philips X-ray powder diffractometer PW/1710 having GIXRD geometry; with Ni filter, using monochromatic CuK radiation of wavelength  $1.5418 \text{ \AA}$  at 50KV and 40mA. The divergence of scanning beam on the source slide was controlled with the help of 0.15mm slit. The specimen were scanned in the range 200 to 800 . Fourier transform infrared spectrometer has been used to study the IR properties of prepared sample in the Mid-IR range, 4000-400  $\text{cm}^{-1}$  using Perkin- Elmer instrument. Absorption spectra of the samples were studied with the help of Lambda 750 (Perkin Elmer) spectrophotometer in the wavelength range of 200–800 nm.

### B. Statistical method and data analysis

The study explored the four main processing parameters in the method of  $Y_2O_3$ - $SiO_2$  was optimized using 3-level, 4-factor central composite experimental design. Concentrations of  $Y_2O_3$ . (x1), concentration of  $SiO_2$ (X2),Annealing temperature(X3) and rotation rate (X4) were used as independent variables on the basis of preliminary trials. Strain was selected as dependent variable and the effect of independent variables on Size and Strain was studied at 3 levels i.e., low (−1), middle (0), high (+1).The experimental design and statistical analysis of data were done using the Design Expert software (version 9.0.6.2). For this study. Experimental conditions for the tests conducted are summarized in Table 1,The Strain of nano particle based on the results of a preliminary set of experiments,

Table 1:-Experimental Design for Strain.

Factors	High level	Medium level	Low level
Con $Y_2O_3$ (X1)	1	0	-1
Con $SiO_2$ (X2)	1	0	-1
Temperature(X3)	1	0	-1
Drop rate(X4)	1	0	-1

Statistical analysis was performed using DesignExpert1 software. In this study, the optimum operation conditions strain was obtained by analyzing the relationships between the variables (con  $Y_2O_3$ ,Con  $SiO_2$ ,Temperature and Drp) and the response (Strain). The behaviour of the RSM in this study was expressed by the following polynomial equation[16-18]

$$Y = + \sum_{i=1}^n A_i X_i + e \quad (1)$$

where Y is the response variable  $A_i$ , represents the linear effect regression terms; n is the number of independent variable; and e is the random error. Coefficient of determination ( $R^2$ ) was used to describe the accuracy of the model; F value (Fisher variation ratio) and probability value (Prob > F) were applied to evaluate the significance of the model terms [16,19]

Design Expert to detect any outlier and unreliable result and collected data was in the acceptable range to be used to develop the

### C. Statistical analysis and modeling

In the Central composite design performing 30runs the experimental results for particle size and strain, data was evaluated by model. Regression analysis was applied to develop the best-fit model using the collected data. In Table2, Design summary by RSM

for central composite experiments design has been given. While in Table 3, data obtained by RSM for strain(Response summary) has been given .

Table2: Design summary:-

		Factor 1	Factor 2	Factor 3	Factor 4	Response 1
Std	Run	A(con y <sub>2</sub> O <sub>3</sub> )	B(con sio <sub>2</sub> ):	C:temperature	D:drp	Strain
		G	g	°c	r/m	---
27	1	-1	0	1	-1	0.000243
1	2	1	-1	0	-1	0.000158
22	3	-1	-1	-1	-1	0.000119
16	4	1	1	1	1	0.000121
17	5	-1	0	0	0	0.000243
29	6	0	0	0	0	0.000443
8	7	1	1	1	-1	0.000589
28	8	0	0	0	0	0.000456
24	9	0	0	0	1	0.000444
21	10	0	0	-1	0	0.000589
20	11	0	1	0	0	0.000456
2	12	1	-1	-1	-1	0.000467
13	13	-1	-1	1	1	0.000378
10	14	1	-1	-1	1	0.000478
23	15	0	0	0	-1	0.000213
11	16	-1	1	-1	1	0.000401
26	17	0	0	0	0	0.000335
9	18	-1	-1	-1	1	0.000571
18	19	1	0	0	0	0.000374
5	20	-1	-1	1	-1	0.000368
6	21	1	-1	1	-1	0.000178
14	22	1	-1	1	1	0.000375
7	23	-1	1	1	-1	0.000215
4	24	1	1	-1	-1	0.000349
3	25	-1	1	-1	-1	0.000568
12	26	1	1	-1	1	0.000459
25	27	0	0	0	0	0.000375
15	28	-1	1	1	1	0.000167
30	29	0	0	0	0	0.000389
19	30	0	-1	0	0	0.000465

Table 3: Response summary.

Resp onse	Name	Unit s	Obs	Analysis	Minimum	Maximum	Mean	Std. Dev.	Ratio	Trans	Model
R1	Strain	---	30	Polynomial	0.00012	0.000589	0.00038283	0.00012526	4.867	Power	Linear

The response Strain (Y1) was predicted by a linear equation shown as Eq. (2) below.

$$Y1=3.828E-004+5.694E-005*X1+5.839E-005*X2+7.050E-005*X3+3.489E-005X4 \text{ ---- (2)}$$

where Y1 is the strain, X1 is the concentration of A, X2 is the concentration of B, X3 is the annealing temperature,X4 is the drop rate per minute .To evaluate the statistical significance of the quadratic model. F-test was conducted for the analysis of variance (ANOVA). The ANOVA tests results for the out put Strain is as shown in Table 4.



### III. RESULT AND DISCUSSION

It is here very difficult to define ANOVA in a simple word precisely but yet we try, We can say that when several ideas are synthesized and they can be used for multiple purposes-ANOVA comes in frame. The collection of statistical models which are used to analyze the differences among group means and the procedures associated with them, For example, "variation" between groups, Ronald Fisher, the father of "ANOVA" was an evolutionary statistician and biologist. In the ANOVA, the observed variance in a particular variable, partitioned into components attributable to different sources of variation. ANOVA provides a statistical test which is used to check whether or not the means of several groups are equal and then generalizes the t-test to more than two groups. It is also used to compare three or more groups or variables for statistical significance. suited to a wide range of practical problems. ANOVA, a particular form of statistical hypothesis testing strongly used in the analysis of experimental data. A when a probability (p-value) comes out to be less than a threshold (significance level) now this type of result become statistically significant, justifies the rejection of the null hypothesis( all groups are simply random samples of the same population). In short, we can say that ANOVA is a statistical tool, which can be used in several ways to develop and confirm an explanation for the observed data. we can also do the given things with the help of ANOVA. It is computationally elegant, relatively robust against violations of its assumptions. With the help of ANOVA, multiple samples can be compared ( statistical analysis). In the same way, it can also be used to analysis of a variety of experimental designs. ANOVA "is probably the most useful technique in the field of statistical inference. To obtain the difference between the variance of observations and the variance of means the result multiplied by the number of observations in each treatment,

Table 4: for ANOVA for Response Surface linear model..

ANOVA for Response Surface Linear model						
Analysis of variance table [Partial sum of squares - Type III]						
	Sum of		Mean	F	p-value	
Source	Squares	Df	Square	Value	Prob > F	
Model	2.311E-007	4	5.778E-008	6.45	0.0010	Significant
X1-con A	5.837E-008	1	5.837E-008	6.52	0.0172	
X2-con B	6.137E-008	1	6.137E-008	6.85	0.0148	
X3-temperature	8.946E-008	1	8.946E-008	9.99	0.0041	
X4-drp	2.191E-008	1	2.191E-008	2.45	0.1304	
Residual	2.239E-007	25	8.957E-009			
Lack of Fit	1.918E-007	20	9.589E-009	1.49	0.3495	not significant
Pure Error	3.214E-008	5	6.428E-009			
Cor Total	4.550E-007	29				

The fundamental technique deviding the total sum of squares (SS) into components related to the effects used in the model. For example, the model for a simplified ANOVA with one type of treatment at different levels. The number of degrees of freedom (DF) , partitioned in a similar way: one of these components (that for error) specifies a chi-squared distribution describes the associated sum of squares, while the same is true for "treatments" if there is no treatment effect. F-test can be used in ways like F-test can be used in both therefore one-way or single-factor ANOVA. By comparing the F-test statistic we can test statistical significance. The critical value of F is a function of the degrees of freedom of the numerator and the denominator and the

significance level depends upon the ( $\alpha$ ). Null hypothesis rejected only in case where  $F \geq F_{\text{Critical}}$ . The null hypothesis can also be rejected if probability is less than or equal to the significance level ( $\alpha$ ). F-test can be considered to be nearly optimal, to minimize false negative errors for a fixed rate of false positive errors (i.e. maximizing power for a fixed significance level). The F-test's p-values nearly approximate the permutation test's p-values. The approximation is particularly close when the design is balanced. Probability Values (p-Values) Probability values ( $P$ -values) It does not necessarily measure the importance of a regressor. An important regressor may have a large (nonsignificant)  $P$ -value if the sample is small, if the regressor calculated over a narrow range, For large measurement errors, or another closely related regressor can included in the equation. An unimportant regressor always have a very small  $P$ -value in a large sample. Computing a confidence interval for a parameter estimate gives you more useful information than just looking at the  $P$ -value, but confidence intervals can not solve problems of measurement errors in the regressors or highly correlated regressors.

Table 5 : Coefficient of determination ( $R^2$ ), (ANOVA test result).

Std. dev	9.464E-005	R-Squared	0.5079
Mean	3.828E-004	Adj. R- Squared	0.4292
C.V. %	24.72	Pred. R-Squared	0.3347
PRESS	3.027E-007	Adeq. Precision	11.4267

Coefficient of determination ( $R^2$ ), adjusted  $R^2$  and predicted  $R^2$  values were used to evaluate the fitness of the model. Adjusted  $R^2$ , which adjusts for the number of explanatory terms in a model relative to the number of data points. It is the is a modification of  $R^2$  [16-20]. How well a regression model predicts responses for new observations is represented by, The predicted  $R^2$  [21]. The residual error to the pure error from triplicated experimental design points are compared by the lack of fit. In model, the p-value for lack-of-fit is 0.3495, which is greater than 0.0010, indicating that the lack-of-fit is not significant relative to the pure error. However, a model with reasonable  $R^2$  value is acceptable with significant lack-of-fit [22-24]. Table 5 gives information regarding data for Coefficient of determination ( $R^2$ ), (ANOVA test result). The Model F-value of 6.45 implies the model is significant. There is only a 0.10% chance that an F-value this large could occur due to noise. Values of "Prob > F" less than 0.0500 indicate model terms are significant. In this case  $X_1, X_2, X_3$  are significant model terms. Values greater than 0.1000 indicate the model terms are not significant. The "Pred R-Squared" of 0.3347 is in reasonable agreement with the "Adj R-Squared" of 0.4292; i.e. the difference is less than 0.2. "Adeq Precision" measures the signal to noise ratio. A ratio greater than 4 is desirable, ratio of 11.426 indicates an adequate signal. This model can be used to navigate the design space. The red line was produced by the software based on the externally studentized to define outliers, as shown in the diagnostics plots outlier exists in the plot indicating that the model is consistent with all the data. All the externally studentized residual were randomly scattered across the graph and Furthermore, there is no significant distribution pattern for all the diagnostics plots graphs. The residuals are normally distributed if the points on the plot follow a straight line [25] Normal probability plot of the studentized residuals to check for normality of residuals. Studentized residuals versus predicted values to check for constant error. Externally Studentized Residuals to look for outliers, i.e., influential values. Box-Cox plot for power transformations. A three-dimensional surface plot Figs. respectively, to provide a better visualization of the statistically significant factors derived from the statistical analysis.

Design-Expert® Software  
(strain)<sup>1</sup>  
Color points by value of  
(strain)<sup>1</sup>:  
0.001  
0.000

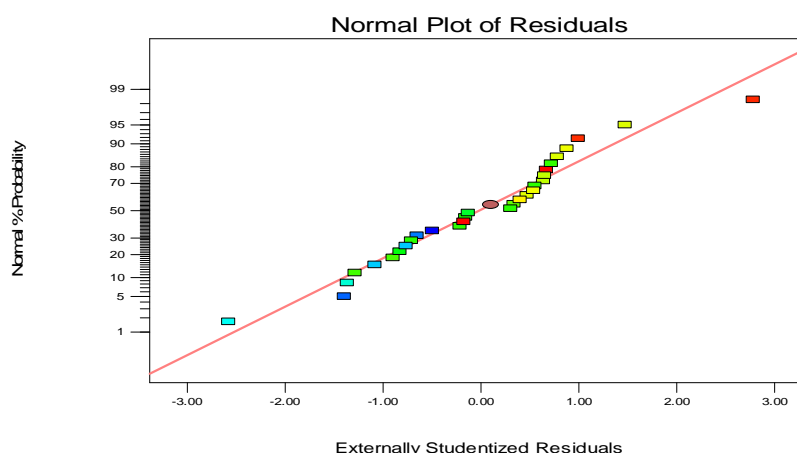


Fig1: Normal plot of Residuals (Externally Studentized).

The red line was produced by the software based on the externally studentized to define outliers as shown in the diagnostics plots Fig.(1-5). The outlier exists in the plot indicating that the model is consistent with all the data. All the externally studentized residual were randomly scattered across the graph and furthermore, there is no significant distribution pattern for all the diagnostics plots/graphs. The residuals are normally distributed if the points on the plot follow a straight line. Normal probability plot of the studentized residuals are to check for normality of residuals. Studentized residuals versus predicted values are to check for constant error. Externally Studentized residuals are to look for outliers, i.e., influential values.

Design-Expert® Software  
(strain)\*1

Color points by value of  
(strain)\*1:  
0.001  
0.000

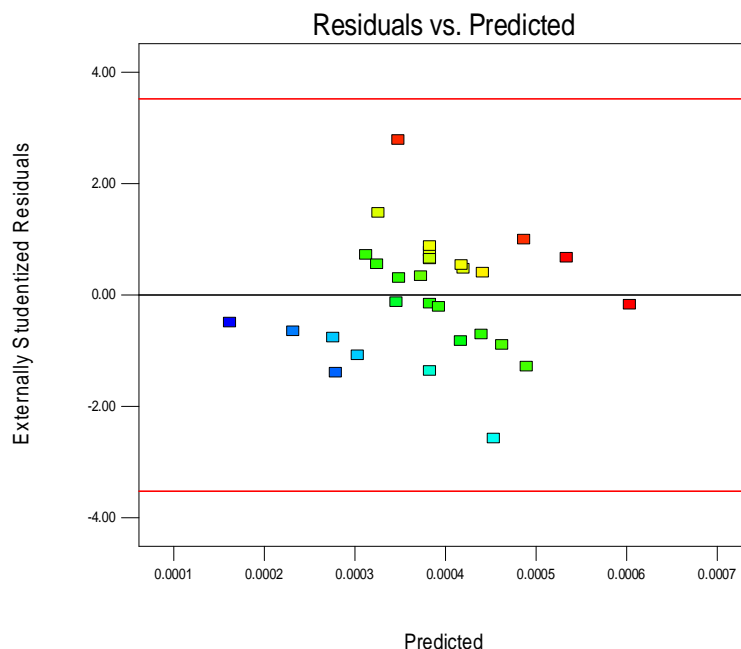


Fig2:Residuals vs. Predicted(Externally studentized)

After the model has been fitted, predicted and residual values are calculated, graphed, and output. The predicted values, calculated from the estimated regression equation; the raw residuals were calculated as the observed minus the predicted value. Often other forms of residuals were used for model diagnostics, such as studentized or cumulative residuals. Some procedures may calculate predicted mean values, standard errors of residuals and individual predicted values.

Let one may consider the observation of which is the row of regressors, is the vector of parameter estimate and for the residual variance (the mean squared error) it is  $S^2$ . The leverage value of the observation is defined as

$$h_i = w_i x_i' (x' w x)^{-1} x_i$$

where  $x$  is the design matrix for the observed data,  $x_i'$  is an arbitrary regressor vector (possibly but not necessarily a row of  $x$ ),  $w$  is a diagonal matrix with the observed weights on the diagonal, and  $w_i$  is the weight corresponding to  $x_i'$ .

Then the predicted mean and the standard error of the predicted mean are

$$\hat{Y}_i = x_i' \beta$$

$$STDERR(\hat{Y}_i) = \sqrt{(s^2 h_i / w_i)}$$

The standard error of the individual (future) predicted value  $y_i$  can be calculated as

$$STDERR(y_i) = \sqrt{s^2 (1 + h_i) / w_i}$$

If the predictor vector  $x_i$  corresponds to an observation in the analysis data, then the raw residual for that observation and the standard error of the raw residual are defined as

$$RESID_i = Y_i - \hat{Y}_i = x_i' \beta$$

$$STDERR(RESID_i) = \sqrt{s^2 (1 - h_i) / w_i}$$

In the case where model assumptions may be reasonable in that situation Residuals, will appear to be normally distributed, close to statistically independent and have a constant variance. It will not differ for different treatment groups

Design-Expert® Software  
(strain)<sup>1</sup>

Color points by value of  
(strain)<sup>1</sup>:  
0.001  
0.000

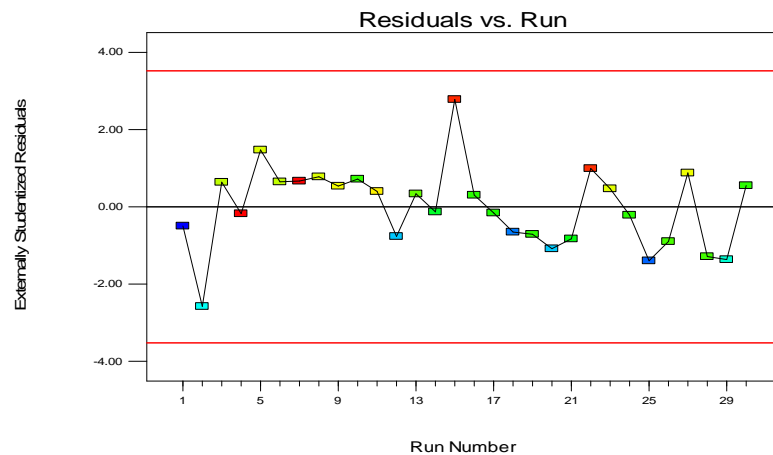


Fig3:Residual vs. Run Number(Externally studentized).

Design-Expert® Software  
(strain)<sup>1</sup>

Color points by value of  
(strain)<sup>1</sup>:  
0.001  
0.000

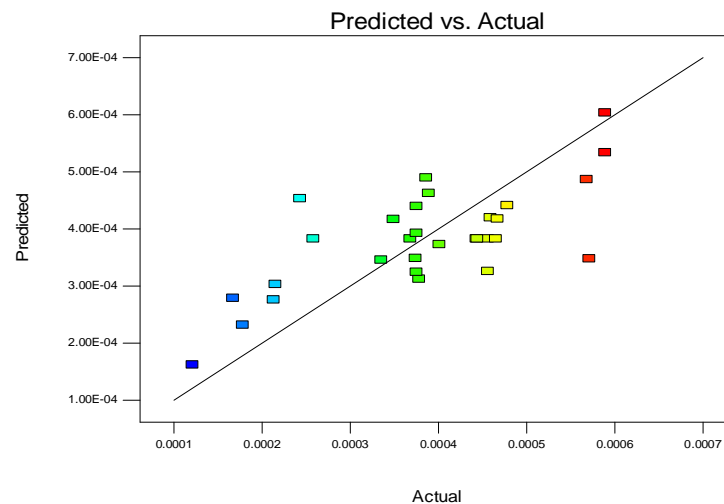


Fig4: predicted versus Actual.

Design-Expert® Software  
(strain)<sup>1</sup>

Lambda  
Current = 1  
Best = 1.03  
Low C.I. = 0.1  
High C.I. = 2.06

Recommend transform:  
None  
(Lambda = 1)

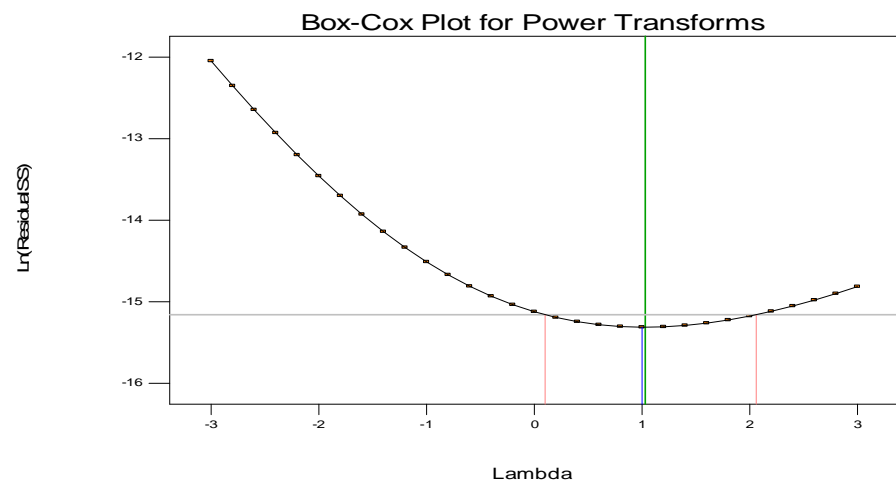


Fig5:Box-Cox Plot for Power transforms(Ln of Residual/Lambda).



The assumption of normality are followed by many statistical tests and intervals . The assumption of normality often leads to those tests which are simple, mathematically tractable, and powerful compared to tests that do not make the normality assumption. But some time, many real data sets are in fact not normal. In Table 6 dta for Box-cox Power Transformation has been given. However, an appropriate transformation of a data set may often yield a data set that follows a normal distribution. This increases the applicability and usefulness of statistical techniques based on the normality assumption. The correlation computed between the vertical and horizontal axis variables of the probability plot and is a convenient measure of the linearity of the probability plot and we know that the more linear the probability plot, the better a normal distribution fits the data

Table 6:Box-cox Power Transformation

Box-Cox Power Transformation Constant	95% CI	95% CI	Best	Rec.
k	Low	High	Lambda	Transform
0.000	0.100	2.06	1.03	None

#### A. XRD

X-ray crystallography is a tool used for identifying the atomic and molecular structure of crystal, in which the crystalline atoms cause a beam of incident X-rays to diffract into many specific directions. XRD results of the samples annealed at different annealing conditions have been shown in Fig(16). The fig.6, shows the diffraction peaks at  $2\theta \sim 20.62^\circ$  (211),  $29.30^\circ$  (222),  $33.94^\circ$  (400),  $36.06^\circ$  (411),  $38.06^\circ$  (420),  $40^\circ$  (332),  $43.64^\circ$  (134),  $47.06^\circ$  (521),  $48.68^\circ$  (440),  $50.28^\circ$  (433),  $53.36^\circ$  (611),  $56.32^\circ$  (145),  $57.76^\circ$  (622),  $59.18^\circ$  (136),  $60.58^\circ$  (444),  $62^\circ$  (543),  $63.38^\circ$  (046),  $64.66^\circ$  (721). These peaks shows the cubic structure of  $Y_2O_3$  [JCPDS file no. 741828].

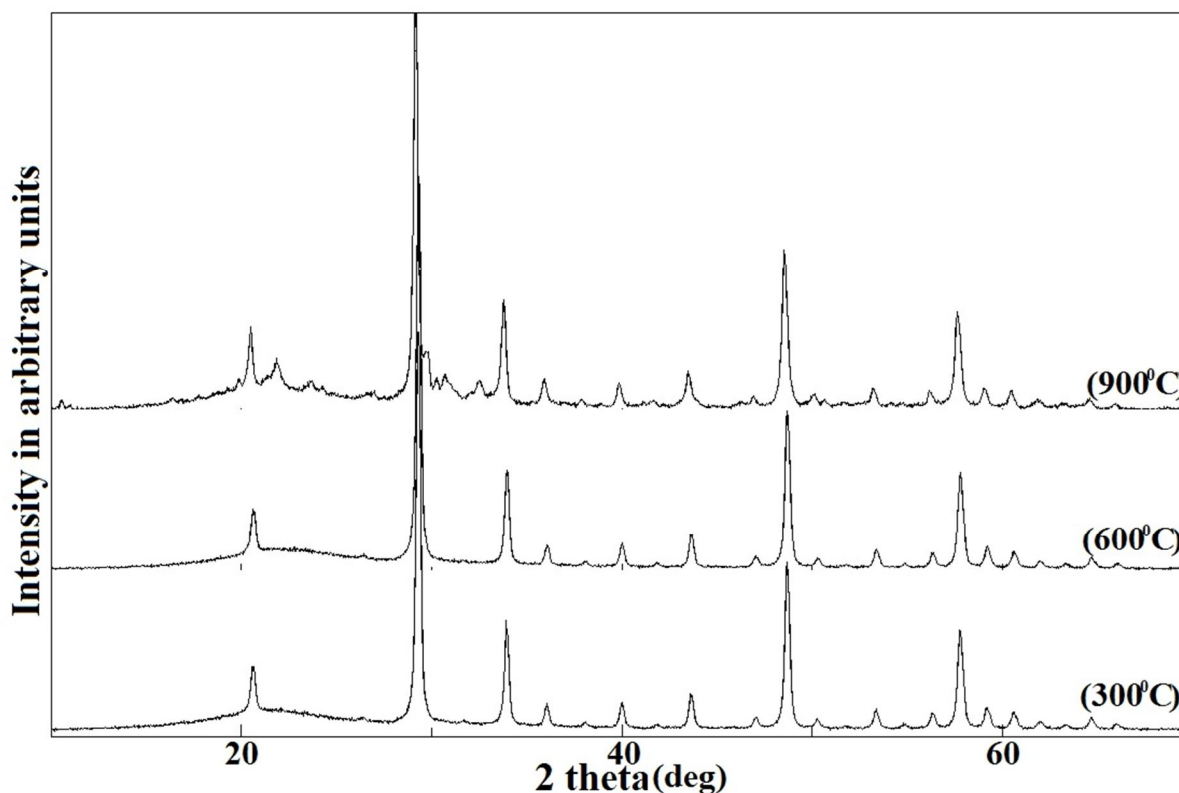


Fig.6 : XRD pattren of sample annealed at temperature 300°C, 600°C, 900°C. showing sharpning of peak at higher temperature.

#### B. FTIR

Fourier transform infrared spectroscopy is a technique which enables us to identify the organic, inorganic materials and specially the presence of impurity phase in natural or synthesized materials. Fig (7) shows the FTIR spectrum of as prepared  $Y_2O_3/SiO_2$ . The peaks at  $3447.07\text{ cm}^{-1}$  assigned to the stretching vibration of H–O–H. The absorption bands around  $1636.16\text{ cm}^{-1}$  due to bending of H–O–H absorbed at silica surface. The two medium absorption bands around  $799.14\text{ cm}^{-1}$  and  $467.18\text{ cm}^{-1}$  are attribute to

symmetric stretching and bending vibrations of Si-O-Si bond. Band appeared around  $563.01\text{ cm}^{-1}$  attribute to stretching vibrations of Y-O bond [10,11]. The FTIR spectrum of  $\text{Y}_2\text{O}_3/\text{SiO}_2$  annealed at  $900^\circ\text{C}$  shows in the fig (7). In this fig. peak at  $3422.71\text{ cm}^{-1}$  shows several broad absorption band of the O-H. Peak at  $1108.16\text{ cm}^{-1}$  and  $801.49\text{ cm}^{-1}$  due to the symmetric and asymmetric stretching vibrations of Si-O-Si bond.

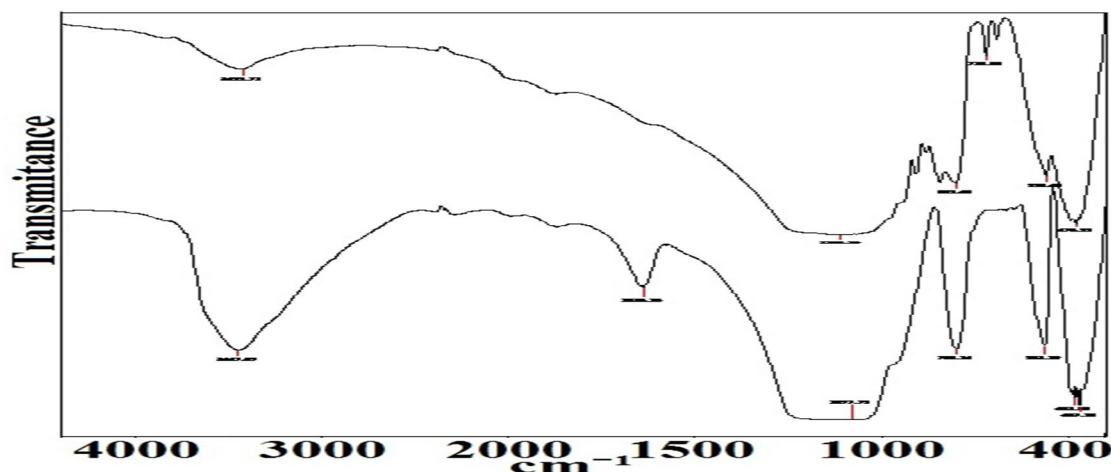


Fig. 7: FTIR

#### IV. CONCLUSION

Nanocrystalline  $\text{Y}_2\text{O}_3/\text{SiO}_2$  powder with average size of 28 nm has been effectively prepared by chemical coprecipitation method. The cubic nature of yttria nanoparticles with crystalline silica is confirmed by XRD. The strain effect in peak broadening is calculated by W-H Plot. FTIR spectrum of samples analyzed the functional group and characteristic bond of the used precursors. Data were analyzed using Design Expert\_ version 9.0.6.2 software. The significant effect of independent factors were analyzed using ANOVA. The Model F-value of 6.45 (for strain) implies the model is significant. The correlation coefficient of determination  $R^2$  was 0.5079 for strain indicating that the observed results fitted well with the model prediction, and the effect was also reported in the form of 3D perturbation plots. From 3D plot we concluded that size of particle is strongly affected by concentration and temperature and strain is affected by drop rate and concentration of  $\text{SiO}_2$ .

#### V. ACKNOWLEDGMENT

We are deeply grateful to Director of the T.I.T. Institution. He gives insightful comments and suggestions. I am particularly grateful for the assistance given by the Puran sir.

#### REFERENCES

- [1] T.B. Troczynski, P.S. Nicholson, "Effect of Additives on the pressure less sintering of aluminum nitride between  $1500$  and  $1800^\circ\text{C}$ ", J. Am. Ceram. Soc. 72, 1488–1491, 1989.
- [2] A.H. Kitai, "Oxide phosphor and dielectric thin films for electroluminescent devices", Thin Solid Films 445, 367–376, 2003.
- [3] G. Yao, L.B. Su, J. Xu, X.D. Xu, L.H. Zheng, Y. Cheng, "Spray combustion synthesis of nanocrystalline  $\text{Y}_2\text{O}_3$  and its thermodynamical and morphological study", J. Cryst. Growth 310, 404–409, 2008.
- [4] Xiaozhen Ren, Lizhu Tong, Xiaodong Chen, Hong Ding, Hua Yang, "Fabrication, magnetic and luminescent properties of  $\text{CoFe}_2\text{O}_4/\text{SiO}_2/\text{Y}_2\text{O}_3:\text{Dy}^{3+}$  composites" Journal of Alloys and Compounds 589, 76–81, 2014
- [5] E. M. Levin, C. R. Robbins, and H. F. McMurdie, "Phase Diagrams for Ceramists 1969 Supplement, The American Ceramic Society", Inc., Columbus, OH; Fig. 2388.
- [6] R. Chaim, A. Shpayer, C. Estournes, "Densification of nanocrystalline  $\text{Y}_2\text{O}_3$  ceramic powder by spark plasma sintering", J. Eur. Ceram. Soc 29, 91–98, 2009.
- [7] P. Aghamkar, S. Duhan, M. Singh, N. Kishore, P.K. Sen, "Effect of thermal annealing on  $\text{Nd}_2\text{O}_3$ -doped silica powder prepared by the sol-gel process", J. Sol-Gel Sci. Technol. 46, 17–22, 2008.
- [8] K. Takaichi, J. Lu, T. Murai, T. Uematsu, K. Ueda, H. Yagi, T. Yanagitani, A.A. Kaminskii, "Chromium doped  $\text{Y}_3\text{Al}_5\text{O}_{12}$  ceramics - a novel saturable absorber for passively Q-switched one-micron solid state lasers Jpn.", J. Appl. Phys., vol.41, L96-L98, 2002.
- [9] R. Schmechel, M. Kenedy, H. Von Seggem, H. Winkler, M. Kolbe, R.A. Fischer, R.A. Fischer, Li Xiaomao, A. Benker, M. Winterer, "Luminescence properties of nanocrystalline  $\text{Y}_2\text{O}_3:\text{Eu}^{3+}$  in different host materials", J. Appl. Phys. 89, 1679, 2001.
- [10] Q. Li, L. Gao, D. Yan, "Effects of the Coating Process on nanoscale  $\text{Y}_2\text{O}_3:\text{Eu}^{3+}$  powder", J. Chem. Mater. 11(1999) 533, 1999.
- [11] W. E. Lee, C. H. Drummond III, G. E. Hilmas, J. D. Kiser, and W. A. Sanders, "Microstructural Evolution on Crystallizing the Glassy Phase in a 6 Weight %  $\text{Y}_2\text{O}_3$ - $\text{Si}_3\text{N}_4$  Ceramic," these proceedings.



- [12] R.K.Deshmukh, J.B Naik, "Diclofenac sodium-loaded Eudragit® microspheres optimization using statistical experimental design", J Pharm Innov 8:276–287, 2013
- [13] Sharma, A. Malik, S. Satya, "Application of response surface methodology (RSM) for optimization of nutrient supplementation for Cr(VI) removal by *Aspergillus lentulus* AML05", J. Hazard. Mater. 164 (2), 1198–1204, 2009.
- [14] D.C.Montgomery, Design and Analysis of Experiments, fifth ed., Wiley, New York, John Wiley & Sons, New Jersey, 2001.
- [15] W. E. Lee, C. H. Drummond III, G. E. Hilmas, J. D. Kiser, and W. A. Sanders, "Microstructural Evolution on Crystallizing the Glassy Phase in a 6 Weight %  $\text{Y}_2\text{O}_3$ -Si $_3\text{N}_4$  Ceramic," these proceedings.
- [16] Y. Ding, M. Sartaj, "Statistical analysis and optimization of ammonia removal from aqueous solution by zeolite using factorial design and response surface methodology", J. Environ. Chem. Eng. 3 (2), 807–814, 2015.
- [17] X. Zhu, J. Tian, R. Liu, L. Chen, "Optimization of Fenton and electro-Fenton oxidation of biologically treated coking wastewater using response surface methodology", Sep. Purif. Technol. 81 (3), 444–450, 2011.
- [18] F. Gomez, M. Sartaj, "Optimization of field scale biopiles for bioremediation of petroleum hydrocarbon contaminated soil at low temperature conditions by response surface methodology (RSM)", Int. Biodeterior. Biodegrad. 89, 103–109, 2014.
- [19] D.C. Montgomery, Design and Analysis of Experiments, John Wiley & Sons, 2008.
- [20] M.J Anderson, P.J. Whitcomb, "RSM Simplified: Optimizing Processes Using Response Surface Methods for Design of Experiments", Productivity Press, 2005.
- [21] R.H. Myers, D.C. Montgomery, C.M. Anderson-Cook, "Response Surface Methodology: Process and Product Optimization Using Designed Experiments", vol. 705, John Wiley & Sons, 2009.
- [22] H. Jabeen, et al., "Optimization of profenofos degradation by a novel bacterial consortium PBAC using response surface methodology", Int. Biodeterior. Biodegrad. 100, 89–97, 2015.
- [23] N. Benyahia, N. Belkhouche, J.Å. Jönsson, "A comparative study of experimental optimization and response surface methodology of Bi(III) extraction by emulsion organophosphorus liquid membrane", J. Environ. Chem. Eng. 2 (3), 1756–1766, 2014.
- [24] P. Palaniandy, H.B.A. Aziz, S. Feroz, "Treatment of petroleum wastewater using combination of solar photo-two catalyst  $\text{TiO}_2$  and photo-Fenton process", J. Environ. Chem. Eng. 3 (2), 1117–1124, 2015.
- [25] H. Zhang, X. Ran, X. Wu, D. Zhang, "Evaluation of electro-oxidation of biologically treated landfill leachate using response surface methodology", J. Hazard. Mater. 188, 261–268, 2011.



10.22214/IJRASET



45.98



IMPACT FACTOR:  
7.129



IMPACT FACTOR:  
7.429



# INTERNATIONAL JOURNAL FOR RESEARCH

IN APPLIED SCIENCE & ENGINEERING TECHNOLOGY

Call : 08813907089  (24\*7 Support on Whatsapp)